CONF-820429--9

LA-UR -82-961

MASTER

LA-UR--82-961

DE82 014061

Los Alamos National Laboratory is operated by the University of California for the United States Department of Energy under contract W-7405-ENG-36

TITLE METHODS FOR THE SOLUTION OF THE TWO-DIMENSIONAL RADIATION-TRANSFER EQUATION

AUTHOR(S) Robert Weaver, X-7, Los Alamos National Laboratory
Dimitri Mihalas, X-DO Consultant, Sacramento Peak Observatory
Gordon Olson, X-7, Los Alamos National Laboratory

SUBMITTED TO. Los Alamos/CEA Conference
Paris, France
April 19-23, 1982

Los Alamos Los Alamos National Laboratory
Los Alamos, New Mexico 87545

METHODS FOR THE SOLUTION OF THE TWO-DIMENSIONAL RADIATION TRANSFER EQUATION

by

Robert Weaver,[1] Dimitri Mihalas,[2] Gordon Olson[1]

ABSTRACT

We use the variable Eddington factor (VEF) approximation to solve the time-dependent two-dimensional radiation transfer equation. The transfer equation and its moments are derived for an inertial frame of reference in cylindrical geometry. Using the VEF tensor to close the moment equations, we manipulate them into a combined moment equation that results in an energy equation, which is automatically flux limited.

There are two separable facets in this method of solution. First, given the variable Eddington tensor, we discuss the efficient solution of the combined moment matrix equation. The second facet of the problem is the calculation of the variable Eddington tensor. Several options for this calculation, as well as physical limitations on the use of locally-calculated Eddington factors, are discussed.

---

[1] Group X-7, Los Alamos National Laboratory
[2] X-Division Consultant, Los Alamos National Laboratory

I. INTRODUCTION

In two spatial dimensions, the time-dependent radiation transfer equation is at least a six-dimensional problem $(r,z,t;\theta,\phi,\nu)$. Many classes of methods have been advanced to solve this complex problem, including S_n methods,[1] Feautrier methods,[2] and moment equation expansions,[3] to name a few. In this paper we examine the moment expansion method.

Because angular projection factors appear in the transfer equation itself, this moment expansion technique always produces a system containing more unknowns (moments) than equations to determine them. Thus a closure relation is required. A particularly attractive scheme is to introduce variable Eddington factors to close the system of moment equations.[4] In one spatial dimension, a scalar Eddington factor is all that is required to close the system. However, in two spatial dimensions, the closure requires three independent factors (an Eddington tensor) because the second moment has three independent components (P_{rr}, P_{zz}, and P_{rz}).

The moment method of solving the transfer equation has two separable facets. One needs to solve the system of moment equations, given the closure information; and, given the solution of the moment equations (hence the distribution of sources and sinks), one needs to determine the VEF tensor. In this paper, we discuss briefly the various computational techniques one can use to handle each of these facets of the method.

An important limiting case for the moment equations is obtained if one assumes a constant Eddington factor. In particular, deep within an opaque radiating fluid (e.g., a stellar interior) the radiation field becomes nearly isotropic and steady in time. In this regime, the flow of radiation energy can be approximated very accurately by a diffusion equation. Also the vector flux is proportional to the gradient of the energy density; so radiation tends to flow down the gradient from the hotter side to the cooler side. If one assumes that the diffusion

approximation is valid everywhere, then the Eddington factor is everywhere constant, and the solution of the transfer equation is particularly simple. However, most interesting radiation transfer problems (e.g., a pulsating star; a supernova) span the regime from optically thick to optically thin. In the optically thin regions, the assumption of a constant diffusion value for the Eddington factor is no longer valid. In this case, the radiation field becomes anisotropic (i.e., nonlocal), the time dependence of the radiation field may become important and the direction of the radiative flux may no longer be exactly along the gradient of the energy density. Calculating the magnitude of these differences between diffusion and transport is the essence of using variable Eddington factors instead of a constant factor. Moreover, given that efficient codes exist for the solution of the diffusion equation,[5] this variable Eddington tensor method can be formulated in such a way so as to be a natural extension and improvement of existing diffusion codes.

This paper is organized as follows. In Sec. II, we derive the inertial-frame transfer equation in two-dimensional cylindrical geometry. The moment equations are closed by introducing variable Eddington factors. Examples of boundary conditions are derived. In Sec. III, we couple the radiation moment equations to the material energy equation and briefly review techniques for the efficient solution of the combined moment matrix equation. Finally, in Sec. IV, we review methods for obtaining the variable Eddington factors. In particular, we show results comparing Eddington factors calculated with simple formulae (e.g., Minerbo's[6] or Levermore and Pomraning's[7]) to analytic Eddington factors in simple 1D and 2D geometries.

II. TRANSFER EQUATION AND ITS MOMENTS

A. Geometry

We assume the material is contained in a cylinder of finite length with azimuthal symmetry about the cylinder's axis. We

choose r,ϕ,z as coordinates and assume that all material properties are functions of t,r, and z.

The radiation field in the medium is a function of both position and direction, thus the specific intensity is $I(t,r,z,\underset{\sim}{n})$ where $\underset{\sim}{n}$ is the unit vector

$$\underset{\sim}{n} = \sqrt{1-\mu^2}\,\cos\phi\,\hat{\underset{\sim}{r}} + \sqrt{1-\mu^2}\,\sin\phi\,\hat{\underset{\sim}{\phi}} + \mu\,\hat{\underset{\sim}{z}} \quad . \tag{A.1}$$

Here $\mu = \cos\theta$, where θ is the angle between $\underset{\sim}{n}$ and $\hat{\underset{\sim}{z}}$, and ϕ is the azimuthal angle relative to the local radial direction $\hat{\underset{\sim}{r}}$.

B. Transfer Equation

By following a photon path an elementary distance ds in the coordinate system defined above, it is easy to show that the transfer equation is

$$\frac{1}{c}\frac{\partial I}{\partial t} + \frac{\partial I}{\partial s} = \frac{1}{c}\frac{\partial I}{\partial t} + \sqrt{1-\mu^2}\left[\cos\phi\,\frac{\partial I}{\partial r} + \frac{\sin\phi}{r}\left(\frac{\partial I}{\partial \phi} - \frac{\partial I}{\partial \phi}\right)\right]$$

$$+ \mu\,\frac{\partial I}{\partial z} = \kappa B + S - \chi I \quad . \tag{B.1}$$

Here the total extinction coefficient is $\chi \equiv \kappa + \sigma$, the sum of the absorption coefficient κ and the Thomson scattering coefficient σ, B is the Planck function, and S is the Thomson scattering source term

$$S(\mu,\phi) = \frac{3\sigma}{16\pi}\oint I(\underset{\sim}{n}')\left[1 + (\underset{\sim}{n}\cdot\underset{\sim}{n}')^2\right]d\omega' \quad . \tag{B.2}$$

As usual $\oint$ denotes integration over all solid angles $d\omega = d\mu d\phi$, ϕ ranges from 0 to 2π, and μ ranges from -1 to 1.

Because we assume strict azimuthal symmetry $(\partial I/\partial\phi) \equiv 0$, and this term will be dropped henceforth.

C. Moments and Eddington Factors

Define the following moments of the radiation field: zeroth moment, the radiation energy density:

$$E = \frac{1}{c} \oint I(\underset{\sim}{n}) d\omega \ ; \tag{C.1}$$

first moments, the flux components:

$$F_r = \oint I(\underset{\sim}{n}) n_r d\omega = \oint I(\underset{\sim}{n}) \sqrt{1-\mu^2} \cos\phi d\omega \ , \tag{C.2}$$

$$F_\phi = \oint I(n) n_\phi d\omega = \oint I(\underset{\sim}{n}) \sqrt{1-\mu^2} \sin\phi d\omega \equiv 0 \ , \tag{C.3}$$

and

$$F_z = \oint I(\underset{\sim}{n}) \ n_z d\omega = \oint I(\underset{\sim}{n}) \mu d\omega \ ; \tag{C.4}$$

second moments, the pressure tensor components:

$$P_{rr} = \frac{1}{c} \oint I(\underset{\sim}{n}) n_r n_r d\omega = \frac{1}{c} \oint I(\underset{\sim}{n}) \ (1-\mu^2) \cos^2\phi \ d\omega \ , \tag{C.5}$$

$$P_{r\phi} = \frac{1}{c} \oint I(\underset{\sim}{n}) n_r n_\phi d\omega = \frac{1}{c} \oint I(n)(1-\mu^2) \sin\phi\cos\phi \ d\omega \equiv 0 \ , \tag{C.6}$$

$$P_{rz} = \frac{1}{c} \oint I(\underset{\sim}{n}) n_r n_z d\omega = \frac{1}{c} \oint I(n) \ \mu\sqrt{1-\mu^2} \cos\phi \ d\omega \ , \tag{C.7}$$

$$P_{\phi\phi} = \frac{1}{c} \oint I(\underset{\sim}{n}) n_\phi n_\phi d\omega = \frac{1}{c} \oint I(\underset{\sim}{n})(1-\mu^2) \sin^2\phi \ d\omega \ , \tag{C.8}$$

$$P_{\phi z} = \frac{1}{c} \oint I(\underline{n}) n_\phi n_z d\omega = \frac{1}{c} \oint I(\underline{n}) \mu \sqrt{1-\mu^2} \sin\phi \, d\omega \equiv 0 \ , \quad (C.9)$$

and

$$P_{zz} = \frac{1}{c} \oint I(\underline{n}) n_z n_z d\omega = \frac{1}{c} \oint I(\underline{n}) \mu^2 d\omega \ . \quad (C.10)$$

Note that

$$\text{trace } (\underline{\underline{P}}) = P_{rr} + P_{\phi\phi} + P_{zz} \equiv E \ . \quad (C.11)$$

In order to close the system of moment equations we introduce the tensor variable Eddington factor

$$\underline{\underline{f}} \equiv \underline{\underline{P}}/E \ . \quad (C.12)$$

In solving the moment equations these geometric factors are presumed to be given, either from an approximate formula such as given by Minerbo,[6] or from a direct evaluation by a formal solution (see Sec. IV below). In the present calculation there are only three independent components of $\underline{\underline{f}}$, namely f_{rr}, f_{zz}, and f_{rz}; $f_{\phi\phi}$ follows from Eq. (C.11)

$$f_{\phi\phi} = 1 - f_{rr} - f_{zz} \ . \quad (C.13)$$

The scattering source term can be written in terms of the moments defined above as

$$S(\mu,\phi) = \frac{3c\sigma}{16\pi} \left[E + (1-\mu^2)(\cos^2\phi \, P_{rr} + \sin^2\phi \, P_{\phi\phi}) \right.$$

$$\left. + 2\mu(1-\mu^2)^{1/2} \cos\phi \, P_{rz} + \mu^2 \, P_{zz} \right] \ , \quad (C.14)$$

which can be rewritten as

$$S(\mu,\phi) = \frac{3c\sigma E}{16\pi}\left[1 + (1-\mu^2)\sin^2\phi + (1-\mu^2)(1-2\sin^2)f_{rr}\right.$$

$$\left. + 2\mu(1-\mu^2)^{1/2}\cos\phi f_{rz} + \left[\mu^2 - (1-\mu^2)\sin^2\phi\right]f_{zz}\right] . \quad (C.15)$$

D. Moment Equations

Taking the zeroth moment of the transfer equation by integrating Eq. (B.1) against $d\omega$ we find

$$\frac{\partial E}{\partial t} + \frac{1}{r}\frac{\partial(rF_r)}{\partial r} + \frac{\partial F_z}{\partial z} = \kappa(4\pi B - cE) \quad , \quad (D.1)$$

which is obviously the radiation energy equation. Here we made use of the fact that Thomson scattering is conservative so that

$$\oint \left[S(\underline{n}) - \sigma I(\underline{n})\right]d\omega \equiv 0 \quad . \quad (D.2)$$

Next, taking the radial first moment by integrating Eq. (B.1) against $n_r d\omega$ and using Eq. (C.11) we find

$$\frac{1}{c^2}\frac{\partial F_r}{\partial t} + \frac{\partial P_{rr}}{\partial r} + \frac{2P_{rr}+P_{zz}-E}{r} + \frac{\partial P_{rz}}{\partial z} = -\frac{\chi}{c}F_r \quad , \quad (D.3)$$

which is obviously the radial component of the radiation momentum equation. Here we made use of the fact that for Thomson scattering

$$\oint S(\underline{n})\underline{n}\, d\omega = 0 \quad , \quad (D.4)$$

which is evident on physical grounds, and can be verified by direct calculation from Eq. (C.14) or (C.15).

Finally, taking the axial first moment by integrating Eq. (B.1) against $n_z d\omega$ we find

$$\frac{1}{c^2}\frac{\partial F_z}{\partial t} + \frac{1}{r}\frac{\partial}{\partial r}(rP_{rz}) + \frac{\partial P_{zz}}{\partial z} = -\frac{\chi}{c}F_z \quad . \tag{D.5}$$

Equations (D.3) and (D.5) rewritten in terms of Eddington factors are

$$\frac{1}{c^2}\frac{\partial F_r}{\partial t} + \frac{\partial(f_{rr}E)}{\partial r} + \frac{(2f_{rr}+f_{zz}-1)E}{r} + \frac{\partial(f_{rz}E)}{\partial z} = -\frac{\chi}{c}F_r \quad , \tag{D.6}$$

and

$$\frac{1}{c^2}\frac{\partial F_z}{\partial t} + \frac{1}{r}\frac{\partial(rf_{rz}E)}{\partial r} + \frac{\partial(f_{zz}E)}{\partial z} = -\frac{\chi}{c}F_z \quad . \tag{D.7}$$

E. Configuration Factor

In order to eliminate the undifferentiated term in Eq. (D.6) in a convenient way, define the configuration factor[8] q such that

$$\frac{\partial \ell n q}{\partial r} = \frac{2f_{rr}+f_{zz}-1}{rf_{rr}} \quad , \tag{E.1}$$

or

$$\ell n\,[q(r)] = \int_0^r \left(\frac{2f_{rr}+f_{zz}-1}{r'f_{rr}}\right)dr' \quad . \tag{E.2}$$

Then Eq. (D.6) reduces to

$$\frac{1}{c^2}\frac{\partial F_r}{\partial t} + \frac{1}{q}\frac{\partial}{\partial r}(qf_{rr}E) + \frac{\partial(f_{rz}E)}{\partial z} = -\frac{\chi}{c}F_r \quad , \tag{E.3}$$

which is a more pleasant form for the equation.

Note that $q = q(r,z)$. Also, in the isotropic limit $f_{rr} = f_{zz} = \frac{1}{3}$ and $q = 1$, whereas in the radial streaming limit $f_{rr} = 1$, $f_{zz} = 0$, and $q = (\text{constant})\cdot r$. In the axial streaming limit $f_{rr} = 0$, $f_{zz} = 1$ so q is undefined. To choose the correct value in this case we go back to the basic derivation of Eq. (D.3), where we find that the (1/r) term is really $(P_{rr} - P_{\phi\phi})/r$. Thus $\frac{\partial \ell n q}{\partial r} = [1 - (f_{\phi\phi}/f_{rr})]/r$, and in the axial streaming limit if $f_{zz} = 1 - 2\varepsilon$, we may reasonably expect $f_{rr} = f_{\phi\phi} = \varepsilon$, hence $q = 1$. In practice the value chosen should not matter because if $f_{rr} \equiv 0$, the $\frac{\partial}{\partial r}$ terms vanish anyway.

F. Combined Moment Equation

We now use the two momentum equations to eliminate the flux from the energy equation and thereby obtain a single second-order (parabolic) equation for the energy density. To illustrate the approach we write the vector form of the equations:

$$\frac{\partial E}{\partial t} + \underset{\sim}{\nabla}\cdot\underset{\sim}{F} = \kappa(4\pi B - cE) \tag{F.1}$$

and

$$\frac{1}{c^2}\frac{\partial \underset{\sim}{F}}{\partial t} + \underset{\sim}{\nabla}\cdot(\underset{\approx}{f}E) = -\frac{\chi}{c}\underset{\sim}{F} \quad . \tag{F.2}$$

We now difference Eq. (F.2) in time, leaving the space derivatives in continuous form; for stability we use a fully implicit (backwards Euler) scheme. Thus

$$\frac{\underset{\sim}{F}^{n+1} - \underset{\sim}{F}^{n}}{c^2\,\Delta t} + \underset{\sim}{\nabla}\cdot(\underset{\approx}{f}E^{n+1}) = -\frac{\chi^{n+1}}{c}\underset{\sim}{F}^{n+1} \quad , \tag{F.3}$$

or

$$\underset{\sim}{F}^{n+1} = \frac{-c}{\gamma+\chi^{n+1}}\underset{\sim}{\nabla}\cdot(\underset{\approx}{f}E^{n+1}) + \frac{\gamma}{\gamma+\chi^{n+1}}\underset{\sim}{F}^{n} \quad , \tag{F.4}$$

where $\gamma \equiv 1/c\Delta t$. This equation provides a form of flux limiting.[9]

A finite difference representation of the energy equation is

$$\frac{E^{n+1} - E^n}{\Delta t} = \theta\left[\kappa^{n+1}(4\pi B^{n+1} - cE^{n+1}) - \underset{\sim}{\nabla}\cdot\underset{\sim}{F}^{n+1}\right]$$

$$+ (1 - \theta)\left[\kappa^n(4\pi B^n - cE^n) - \underset{\sim}{\nabla}\cdot\underset{\sim}{F}^n\right] \quad , \qquad (F.5)$$

where $\underset{\sim}{\nabla}\cdot\underset{\sim}{F}$ is to be evaluated using Eq. (F.4). In particular, if we use a fully implicit formula ($\theta = 1$) we have

$$(\gamma + \kappa^{n+1})E^{n+1} + \frac{1}{c}\,\underset{\sim}{\nabla}\cdot\underset{\sim}{F}^{n+1} = \frac{4\pi}{c}\,\kappa^{n+1}\,B^{n+1} + \gamma E^n \quad , \qquad (F.6)$$

or substituting from Eq. (F.4),

$$E^{n+1} - \frac{1}{\gamma+\kappa^{n+1}}\,\underset{\sim}{\nabla}\cdot\left[\frac{1}{(\gamma+\chi^{n+1})}\,\underset{\sim}{\nabla}\cdot(\underset{\approx}{f}E^{n+1})\right] = \frac{4\pi}{c}\,\frac{\kappa^{n+1}B^{n+1}}{\gamma+\kappa^{n+1}}$$

$$+ \frac{\gamma E^n}{\gamma+\kappa^{n+1}} - \frac{\gamma}{c(\gamma+\kappa^{n+1})}\,\underset{\sim}{\nabla}\cdot\left(\frac{\underset{\sim}{F}^n}{\gamma+\chi^{n+1}}\right) \quad . \qquad (F.7)$$

In the limit of high opacity and/or long timesteps, which implies $(\chi/\gamma) = (c\Delta t/\lambda_p) >> 1$, Eq. (F.7) reduces to the diffusion equation

$$E^{n+1} = \frac{4\pi}{c}\,B^{n+1} + \frac{1}{\kappa^{n+1}}\,\underset{\sim}{\nabla}\cdot\left[\frac{1}{\chi^{n+1}}\,\underset{\sim}{\nabla}\cdot(\underset{\approx}{f}E^{n+1})\right] \quad . \qquad (F.8)$$

In the limit of low opacity and/or short timesteps, which implies $\chi/\gamma << 1$, Eq. (F.7) reduces to an approximation to the wave equation:

$$E^{n+1} - (c\Delta t)^2 \underline{\nabla}\cdot[\underline{\nabla}\cdot(\underline{\underline{f}}E^{n+1})] = E^n - \frac{1}{c\gamma}\underline{\nabla}\cdot\underline{F}^n$$

$$= 2E^n - E^{n-1} \qquad (F.9)$$

or

$$c^2 \underline{\nabla}\cdot[\underline{\nabla}\cdot(\underline{\underline{f}}E^{n+1})] = (E^{n+1} - 2E^n + E^{n-1})/\Delta t^2$$

$$= (d^2E/dt^2)^n \quad . \qquad (F.10)$$

In writing the second equality in Eq. (F.9) we used Eq. (F.6) for $\kappa/\gamma << 1$.

Now consider the combined moment equation in component form. Taking backwards time-differences in Eqs. (D.7) and (E.3), we obtain

$$F_r^{n+1} = \left(\frac{\gamma}{\gamma+\chi^{n+1}}\right) F_r^n - \frac{c}{(\gamma+\chi^{n+1})q}\frac{\partial(qf_{rr}E^{n+1})}{\partial r}$$

$$- \frac{c}{(\gamma+\chi^{n+1})}\frac{\partial(f_{rz}E^{n+1})}{\partial z} \quad , \qquad (F.11)$$

and

$$F_z^{n+1} = \left(\frac{\gamma}{\gamma+\chi^{n+1}}\right)F_z^n - \frac{c}{(\gamma+\chi^{n+1})}\frac{1}{r}\frac{\partial(rf_{rz}E^{n+1})}{\partial r}$$

$$- \frac{c}{(\gamma+\chi^{n+1})}\frac{\partial(f_{zz}E^{n+1})}{\partial z} \quad . \qquad (F.12)$$

Taking the backwards time difference of Eq. (D.1) and substituting from Eq. (F.11) and (F.12) we have

$$(\gamma+\kappa^{n+1})E^{n+1} - \frac{1}{r}\frac{\partial}{\partial r}\left[\frac{r}{q(\gamma+\chi^{n+1})}\frac{\partial(qf_{rr}E^{n+1})}{\partial r}\right]$$

$$- \frac{1}{r}\frac{\partial}{\partial r}\left[\frac{1}{(\gamma+\chi^{n+1})}\frac{\partial(rf_{rz}E^{n+1})}{\partial z}\right]$$

$$- \frac{1}{r}\frac{\partial}{\partial z}\left[\frac{1}{(\gamma+\chi^{n+1})}\frac{\partial(rf_{rz}E^{n+1})}{\partial r}\right]$$

$$- \frac{\partial}{\partial z}\left[\frac{1}{(\gamma+\chi^{n+1})}\frac{\partial(f_{zz}E^{n+1})}{\partial z}\right] = \frac{4\pi}{c}\kappa^{n+1}B^{n+1}$$

$$+ \gamma E^{n} - \frac{\gamma}{cr}\frac{\partial}{\partial r}\left(\frac{r\,F_r^n}{\gamma+\chi^{n+1}}\right) - \frac{\gamma}{c}\frac{\partial}{\partial z}\left(\frac{F_z^n}{\gamma+\chi^{n+1}}\right) \quad . \text{(F.13)}$$

Let us define the optical-depth-like variables

$$d\tau_r \equiv (\gamma + \chi^{n+1})dr \quad , \qquad \text{(F.14a)}$$

$$d\tau_r' \equiv q(\gamma + \chi^{n+1})\frac{dr}{r} \qquad \text{(F.14b)}$$

and

$$d\tau_z \equiv (\gamma + \chi^{n+1})dz \qquad \text{(F.14c)}$$

Then Eq. (F.13) can be written

$$\frac{(\gamma+\kappa^{n+1})E^{n+1}}{(\gamma+\chi^{n+1})} - \frac{q}{r^2}\frac{\partial^2}{\partial\tau_r'^2}(qf_{rr}E^{n+1}) - \frac{1}{r}\frac{\partial^2(rf_{rz}E^{n+1})}{\partial\tau_z\partial\tau_r} -$$

$$- \frac{1}{r} \frac{\partial^2 (r f_{rz} E^{n+1})}{\partial \tau_r \partial \tau_z} - \frac{\partial^2 (f_{zz} E^{n+1})}{\partial \tau_z^2}$$

$$= \left(\frac{4\pi}{c} \kappa^{n+1} B^{n+1} + \gamma E^n\right)/(\gamma + \chi^{n+1})$$

$$- \frac{\gamma}{cr} \frac{\partial}{\partial \tau_r} \left(\frac{r F_r^n}{\gamma + \chi^{n+1}}\right) - \frac{\gamma}{c} \frac{\partial}{\partial \tau_z} \left(\frac{F_z^n}{\gamma + \chi^{n+1}}\right) . \qquad (F.15)$$

As was true for the vector form of this equation, [Eq. (F.7)], Eq. (F.15) limits correctly to the diffusion equation and to an approximation of the wave equation. An important property of Eq. (F.15) is that it is possible to obtain second-order accurate representations of all the derivative terms operating on E^{n+1}. The term $\partial^2/\partial\tau_r^2$ and $\partial^2/\partial\tau_z^2$ offer no particular difficulties. The cross derivatives $\partial^2/\partial\tau_r\partial\tau_z$ and $\partial^2/\partial\tau_z\partial\tau_r$ can be evaluated uniquely by assuming that the variable $(rf_{rz}E^{n+1})$ can be represented by a product of second-order Lagrange polynomials in $\Delta\tau_r$ and $\Delta\tau_z$ on the nine-point stencil centered on the point of interest.[2] Note that because the derivatives are to be evaluated along lines of constant r and of constant z, the derivatives do not commute.

G. Boundary Conditions

We now obtain exemplary boundary conditions. Consider first the axis r = 0. From symmetry considerations we know that $F_r \equiv 0$ and $P_{rz} \equiv 0$ on the axis. Therefore from Eq. (E.3) we obtain the very simple boundary condition

$$\left.\frac{\partial (q f_{rr} E)}{\partial r}\right|_{r=0} = 0 \qquad (G.1)$$

Although Eq. (F.15) applies at all interior points (i.e., not on the axis or adjacent to the edges), we cannot apply it in

practice on the cylindrical shell next to the axis because we can not compute a finite value for $d\tau_r'$, as defined in Eq. (F.14b), from r = 0 to r = r_1. To get around this difficulty we can rewrite Eq. (F.13) as follows

$$(\gamma + \kappa^{n+1})E^{n+1} - \frac{\partial}{\partial r}\left[\frac{1}{q(\gamma+\chi^{n+1})}\frac{\partial(qf_{rr}E^{n+1})}{\partial r}\right]$$

$$+ \frac{1}{rq(\gamma+\chi^{n+1})}\frac{\partial(qf_{rr}E^{n+1})}{\partial r}$$

$$- \left\{\text{same terms as in remainder of (F.13)}\right\} \quad . \qquad (G.2)$$

Then defining

$$d\tau_r'' \equiv q(\gamma + \chi^{n+1})dr \quad ,$$

we have

$$\frac{(\gamma+\kappa^{n+1})}{(\gamma+\chi^{n+1})}E^{n+1} - q\frac{\partial^2(qf_{rr}E^{n+1})}{\partial\tau_r''^2} - \frac{1}{r(\gamma+\chi^{n+1})}\frac{\partial(qf_{rr}E^{n+1})}{\partial\tau_r''}$$

$$- \frac{1}{r}\frac{\partial^2(rf_{rz}E^{n+1})}{\partial\tau_z\partial\tau_r} - \frac{1}{r}\frac{\partial^2(rf_{rz}E^{n+1})}{\partial\tau_r\partial\tau_z}$$

$$- \frac{\partial^2(f_{zz}E^{n+1})}{\partial\tau_z^2} = \left(\frac{4\pi}{c}\kappa^{n+1}B^{n+1} + \gamma E^n\right)/(\gamma + \chi^{n+1})$$

$$- \frac{1}{cr}\frac{\partial}{\partial\tau_r}\left(\frac{rF_r^n}{\gamma+\chi^{n+1}}\right) - \frac{1}{c}\frac{\partial}{\partial\tau_z}\left(\frac{\gamma F_z^n}{\gamma+\chi^{n+1}}\right) \quad . \qquad (G.3)$$

This equation applies at all interior points, and may, in fact, be preferable to Eq. (F.15). (Note that the first derivative term can be calculated to second order.) Alternatively, it may be best to use Eq. (G.3) just in the radial zones next to the axis, and use Eq. (F.15) elsewhere.

Let us now formulate the surface boundary conditions. For brevity we consider only the cases of specular and diffuse reflection. The imposed incident field case is treated in detail in another report.[10]

Suppose we have specular reflection at some boundary. Then from ray-by-ray symmetry we know that $F_r(R) \equiv 0$, $F_z(0) \equiv 0$, and $F_z(Z) \equiv 0$ on any of the boundaries where the reflection condition applies. Further, at these boundaries $f_{rz} \equiv 0$. Thus for boundary conditions we would have

$$\frac{\partial(qf_{rr}E)}{\partial r} \equiv 0 \qquad (G.4)$$

at $r = R$ from Eq. (E.3), and

$$\frac{\partial(f_{zz}E)}{\partial z} \equiv 0 \qquad (G.5)$$

from Eq. (D.7) at $z = 0$ and/or $z = Z$.

For diffuse reflection, the physical requirement that the total energy across the boundary is returned (isotropically) again implies $F_r(R) \equiv 0$, $F_z(0) \equiv 0$, and $F_z(Z) \equiv 0$ on the boundaries where the reflection condition applies. But in this case we no longer necessarily have ray-by-ray cancellation, and in general $f_{rz} \neq 0$. Therefore from Eq. (D.7) we have

$$\frac{1}{r}\frac{\partial}{\partial r}(rf_{rz}E) + \frac{\partial(f_{zz}E)}{\partial z} \equiv 0 \qquad (G.6)$$

at $z = 0$ or Z, and from Eq. (E.3) we have

$$\frac{1}{q}\frac{\partial}{\partial r}(qf_{rr}E) + \frac{\partial(f_{rz}E)}{\partial z} \equiv 0 \qquad (G.7)$$

at $r = R$.

III. ENERGY BALANCE

The transfer and moment equations written above apply either to the integrated quantities (energy densities, fluxes, etc.) if the material is grey, or monochromatically if it is nongrey, with a separate set of equations for each frequency. In any case, both the opacities and the thermal source terms depend on the material temperature.

The temperature structure is determined by an energy balance equation, which is of the form

$$\rho\left[\frac{DE_m}{Dt} + p_m\frac{D}{Dt}\left(\frac{1}{\rho}\right)\right] = \int_0^\infty \kappa_\nu(cE_\nu - 4\pi B_\nu)d\nu \quad ,$$

where all material properties are functions of temperature and density. The term on the right-hand side is the net energy input to the material from the radiation field. This equation shows that all the transfer equations are coupled together because the temperature structure that determines any monochromatic radiation field is, in turn, determined by the collective action of all these fields.

In practice the radiative terms in the energy balance equation may dominate both the hydrodynamic work term and input from other sources. Thus, to obtain a mutually consistent temperature structure and radiation field for nongrey material, we must in principle solve the energy equation simultaneously with all the frequency-dependent transfer equations; while this

is feasible in 1D, it is computationally prohibitive in 2D, and we must develop a less costly approach. There are several options one needs to consider in order to obtain a consistent description of the interaction of the radiation field with the material. In this section, we shall merely give an overview of the most obvious methods. It should be noted that the following discussion is purely theoretical; the final proof of the feasibility of any of these methods will be in how computationally efficient they can be made. We have some experience in this respect with regard to the 1D equation;[11] however, to date our experience in 2D is limited.

From the work that has been done in one spatial dimension,[12,4] we think there are two main categories of methods: the multifrequency/grey technique and the full multigroup method.

H. Energy Balance - The Multifrequency/grey Technique

The basic idea of the multifrequency/grey technique originated at System, Science and Software[12] in the late 1960's. Here we review the extension of this method to two spatial dimensions. The heart of the technique is to try to write frequency-integrated moment equations that average correctly over the non-grey opacity. Thus, we use spectral profiles generated in a separate set of monochromatic calculations, and assume that these distributions will be relatively insensitive to changes made in the iteration process required to solve the coupled transfer and energy equations.

To obtain the appropriate equations integrate Eqs. (D.1), (D.7), and (E.3) over frequency. Let

$$e_\nu \equiv E_\nu / \int E_\nu d\nu = E_\nu / E \quad , \tag{H.1}$$

$$b_\nu \equiv B_\nu / \int B_\nu d\nu = B_\nu / b \quad , \tag{H.2}$$

and define the usual Planck mean

$$\kappa_p \equiv \int \kappa_\nu b_\nu d\nu \quad . \tag{H.2}$$

Further, let

$$f_{rr} \equiv \int f_{rr}(\nu)\, e_\nu d\nu \tag{H.4}$$

$$f_{rz} \equiv \int f_{rz}(\nu)\, e_\nu d\nu \tag{H.5}$$

$$f_{zz} \equiv \int f_{zz}(\nu)\, e_\nu d\nu \tag{H.6}$$

$$\kappa_E \equiv \int \kappa_\nu e_\nu d\nu \tag{H.7}$$

$$\chi_r \equiv \int \chi_\nu F_r(\nu) d\nu / \int F_r(\nu) d\nu \tag{H.8}$$

$$\chi_z \equiv \int \chi_\nu F_z(\nu) d\nu / \int F_z(\nu) d\nu \quad . \tag{H.9}$$

Then the frequency-integrated moment equations are

$$\frac{\partial E}{\partial t} + \frac{1}{r}\frac{\partial (rF_r)}{\partial r} + \frac{\partial F_z}{\partial z} = 4\pi\kappa_p B - c\kappa_E E \tag{H.10}$$

$$\frac{1}{c^2}\frac{\partial F_r}{\partial t} + \frac{1}{q}\frac{\partial}{\partial r}(q f_{rr} E) + \frac{\partial (f_{rz} E)}{\partial z} = -\frac{\chi_r}{c} F_r \tag{H.11}$$

$$\frac{1}{c^2}\frac{\partial F_z}{\partial t} + \frac{1}{r}\frac{\partial (r f_{rz} E)}{\partial r} + \frac{\partial (f_{zz} E)}{\partial z} = -\frac{\chi_z}{c} F_z \tag{H.12}$$

The configuration factor q is again defined by Eq. (E.2), but now using the frequency-averaged Eddington factors Eqs. (H.4) through (H.6).

The frequency-integrated energy equation can now be written

$$\rho \left[\frac{DE_m}{Dt} + p_m \frac{D}{Dt}\left(\frac{1}{\rho}\right)\right] = c\kappa_E E - 4\pi\kappa_p B \quad . \tag{H.13}$$

The basic assumption we are making in this approach is that, like the Eddington factors, the ratios e_ν, $F_r(\nu)/F_r$, and $F_z(\nu)/F_z$ can be determined from a frequency-dependent formal solution and then held <u>fixed</u> in the solution of the coupled moment and energy-balance equations.

To obtain a combined moment equation we proceed as before, replacing time derivatives with backward time differences. However, since we wish to present here only a brief discussion of applying this technique in two dimensions, the combined moment equations for the multifrequency/grey technique will not be derived.

It is worth listing the advantages and disadvantages of the multigroup/grey method. The most important single advantage of the method is that it reduces the number of variables used in the energy-balance part of the calculation to an absolute minimum, namely one (the energy density) per meshpoint. This makes the computation of $E(r,z)$ as cheap as possible, and minimizes the cost of iterating the temperature distribution to consistency.

The principal disadvantages of the approach are: (1) We are forced to assume the invariance of the spectral profile functions e_ν, $F_r(\nu)/F_r$, and $F_z(\nu)/F_z$ in the temperature-iteration. In reality the spectral distributions implied by the new temperature distribution at the end of a timestep could be quite different from the initial estimates. The place where this is most serious is in the calculation of κ_g, which determines the total rate of absorption of energy from the radiation field by the material. (2) The formation of flux-weighted mean-free-paths as in Eqs. (H.8) and (H.9) is worrisome, because the directional and frequency distribution of the flux could be such that $\int \chi_\nu F_\nu d\nu$ has the opposite sign from $\int F_\nu d\nu$ (or is zero), which would imply

infinite or negative mean-free-paths in the flux calculation. Both would be unphysical.

I. Energy Balance: The Multigroup Approach

In the direct multigroup approach we assume that at each meshpoint we are going to try to solve simultaneously for the radiation energy density for G groups, plus the temperature. The energy equation to be solved is

$$\rho\left[\frac{DE_m}{Dt} + p_m \frac{D}{Dt}\left(\frac{1}{\rho}\right)\right] = \sum_g w_g \kappa_g (cE_g - 4\pi B_g) \quad . \tag{I.1}$$

Here w_g is the quadrature weight for group g and all material properties are functions of (ρ,T); that is, $E_m = E_m(\rho,T)$, $p_m = p_m(\rho,T)$, $\kappa_g = \kappa_g(\rho,T)$, $B_g = B_g(T)$. Thus we have a nonlinear system (coupled with the transfer equations) to solve. In writing a difference approximation we use fully implicit differencing and evaluate the right-hand side at t^{n+1} for stability.

To solve the system we assume that at each meshpoint we have an estimate T* of the temperature and write $T^{n+1} = T^* + \delta T$, and then linearize all equations for δT. For the present, we will take the simplest possible approach and linearize only E_m and B; we can add other terms if needed later. But in any event the structure of the system is unchanged. We then have

$$\rho\left[\frac{E_m(T^*)+C_V(T^*)\delta T - E_m(T)}{\Delta t} + v_r \frac{\partial E_m(T^*)}{\partial r} + v_z \frac{\partial E_m(T^*)}{\partial z} + p_m(T^*)\frac{D}{Dt}\left(\frac{1}{\rho}\right)\right]$$

$$= -\left[4\pi \sum_g w_g \kappa_g(T^*) \frac{\partial B_g(T^*)}{\partial T}\right]\delta T + \sum_g w_g \kappa_g(T^*)\left[cE_g^{n+1} - 4\pi B_g(T^*)\right] \quad . \tag{I.2}$$

We can solve this equation for δT and write

$$\alpha\, \delta T = \sum_g \beta_g E_g^{n+1} + \gamma \quad , \tag{I.3}$$

where

$$\alpha \equiv \frac{\rho C_V(T^*)}{\partial t} + 4\pi \sum_g \omega_g \kappa_g(T^*) \frac{\partial B_g(T^*)}{\partial t} \tag{I.4}$$

$$\beta_g = c w_g \kappa_g(T^*) \tag{I.5}$$

and

$$\gamma = -\rho\left[\frac{E_m(T^*)-E_m(T^n)}{\Delta t} + v_r \frac{\partial E_m(T^*)}{\partial r} + v_z \frac{\partial E_m(T^*)}{\partial z} + p_m(T^*)\frac{D}{Dt}\left(\frac{1}{\rho}\right)\right]$$

$$- 4\pi \sum w_g \kappa_g(T^*) B_g(T^*) \quad . \tag{I.6}$$

To couple the energy balance into the transfer equation we linearize the source terms in the latter, writing for each group

$$\left(\frac{\gamma+\kappa^*}{\gamma+\chi^*}\right)E^{n+1} - \frac{q}{r^2}\frac{\partial^2 (q f_{rr} E^{n+1})}{\partial \tau_r^2} - \frac{1}{r}\frac{\partial^2 (r f_{rz} E^{n+1})}{\partial \tau_z \partial \tau_r}$$

$$- \frac{1}{r}\frac{\partial^2 (r f_{rz} E^{n+1})}{\partial \tau_r \partial \tau_z} - \frac{\partial^2 (f_{zz} E^{n+1})}{\partial \tau_z^2}$$

$$= \frac{\left(\frac{4\pi}{c}\kappa^* \frac{\partial B^*}{\partial T}\right)\delta T}{(\gamma+\chi^*)} + \frac{\frac{4\pi}{c}\kappa^* B^* + \gamma E^n}{(\gamma+\chi^*)}$$

$$- \frac{\gamma}{c}\left[\frac{1}{r}\frac{\partial}{\partial \tau_r}\left(\frac{r F_r^n}{\gamma+\chi^n}\right) + \frac{\partial}{\partial \tau_z}\left(\frac{F_z^n}{\gamma+\chi^*}\right)\right] \quad . \tag{I.7}$$

Here * on any quantity means that quantity is evaluated at $T = T^*$. Again it should be noted that we have linearized only the Planck function. If we are willing to do the work, we could also linearize κ, χ, and the differential operators.

Equations (I.3) and (I.7) provide a linear system for E_g, (g=1,...,G) and δT at all meshpoints. The first problem (addressed below), is how we solve this big system. Given that we have, we apply δT everywhere, update the material properties, and do the solution over again, iterating to consistency. The iteration may be slower than a full-scale linearization, but it is much simpler, and avoids problems with noisy derivatives.

Let us now map out the form of the grand matrix for the system to be solved. In labeling the energy densities we write E_{ijg} for $E(r_i, z_j, \nu_g)$. From our 1D experience,[11] we expect that the best way to organize the variables and hence the structure of the resulting matrix is to put all frequency groups and the temperature perturbation together at each mesh point. The form of the grand matrix is shown on Fig. 1. Here, at each gridpoint we have an "arrow matrix", which describes the coupling of δT to the local values of E_{ijg} for all groups, and the local response of the radiation fields to δT. These matrices are bordered by a block tridiagonal pattern of diagonal matrices that give the coupling of a given meshpoint to its two adjacent neighbors at the same z-level, and this pattern is in turn bordered by two more tridiagonal blocks of diagonal matrices giving the coupling to meshpoints at the z-levels above and below the current one.

Conceptually, one can view this scheme as emphasizing the frequency coupling at a given spatial point to the local temperature, while handling the spatial coupling to adjacent meshpoints in the outer structure. This scheme is thus well adapted to the optically thick limit because as $\kappa \to \infty$, the diagonal matrices bordering the arrow matrices and the diagonal matrices in bordering squares of the checkerboard all vanish. We realize this advantage only if we actually solve the arrow matrix directly. Happily the decomposition and solution of the matrix is simple:[11]

Consider the matrix

$$A \equiv \begin{pmatrix} & & a_{1I} \\ & \ddots & \vdots \\ & & a_{I-1,I} \\ a_{I1} & \cdots & a_{II} \end{pmatrix} .$$

This matrix can be <u>decomposed</u> into $A = L \cdot U$ where

$$L = \begin{pmatrix} \ell_{11} & & \\ & \ddots & \\ \ell_{I1} & \cdots & \ell_{II} \end{pmatrix} \quad \text{and} \quad U = \begin{pmatrix} 1 & & u_{1I} \\ & \ddots & \vdots \\ & & 1 \end{pmatrix} .$$

Take $u_{ii} \equiv 1$ for $i=1,\ldots,I$. Then $\ell_{ii} = a_{ii}$ for $i=1,\ldots I-1$ and $U_{iI} = a_{iI}/a_{ii}$ for $i=1,\ldots,I-1$. Further, $\ell_{Ij} = a_{Ij}$ for $j=1,..,I-1$ and

$$\ell_{II} = a_{II} - \sum_{j=1}^{I-1} \ell_{Ij} u_{jI} = a_{II} - \sum_{j=1}^{I-1} a_{Ij} u_{jI} \quad . \tag{I.8}$$

So in short, we can form the decompoaition trivially by scaling each element of the last column by $(1/a_{ii})$ to get u_{iI} and accumulating $- a_{Ii} u_{iI}$ into a_{II} to form ℓ_{II}. This is inexpensive, being proportional to I. To <u>solve</u> $Ay = 4$ we then proceed as follows: Consider $L x = R$. Then for $i=1,\ldots,I-1$, $x_i = R_i/\ell_{ii}$ and for $i=I$,

$$x_I = (R_I - \sum_{j=1}^{I-1} \ell_{ij} x_j)/\ell_{II} \quad .$$

Next consider $Uy = x$.

The solution is

$$Y_I = x_I \quad \text{and} \quad y_i = x_i - u_{iI}x_I \quad \text{for} \quad i=1,\ldots,I-1 \quad .$$

NOTE: These decompositions and solutions could be vectorized over all $N_r N_z$ gridpoints. Thus the solution of the overall system, including direct solutions of the arrow matrices down the diagonal, scales as (number of iterations)$\cdot N_r N_z N_g$.

Having solved the system, then, as before, we know E and δT at all gridpoints. We can then update $T^* \rightarrow T^* + \delta T$ and iterate to convergence. The only assumption built into multigroup approach is that Eddington factors remain constant.

J. Energy Balance: Proposed Solution of the Matrix Equation

Consider now the problem of solving the 2D grand matrix equation to obtain E_{ijg} and δT_{ij}. We treat here the grand matrix corresponding to the full multigroup method as developed in Sec. I [i.e., Eqs. (I.3) and (I.7)]; however, the general procedures can be applied to any large, sparse system derived from the transfer equation.

Although a direct solution of the grand matrix equation may be possible, it is computationally much more efficient to use an iterative scheme.[11] In the overall solution, these iterations are the inner iterations to find the value of the temperature correction for each meshpoint. The outer iterations involve applying this temperature correction to make the radiation field consistent with the temperature structure at the advanced time level.

Let us write symbolically the matrix for each r-level represented in Fig. 1 as $\underline{\underline{T}}_i$. Then, we can write the matrix equation corresponding to Eqs. (I.7) and (I.3) as

$$\underline{\underline{T}}_i \; \underline{\Psi}_i = \underline{R}_i \qquad \text{(J.1)}$$

where the vector $\underset{\sim}{\psi}_i \equiv (E_{ijg}, \delta T_{ij}; g=1,\ldots,G; j=1,\ldots,J)$ and $\underset{\sim}{R}_i$ is the resulting right hand side (RHS). The simplest iteration procedure that can be used to solve Eq. (J.1) is to move all the the elements of $\underset{\sim}{T}_i$ to the RHS except the arrow matrices down the main block diagonal (see Fig. 1). The resulting matrix blocks can be decomposed directly and the iteration scheme would be very efficient for cells that are optically thick.[11] For optically thin cells, the number of iterations may become excessive for such a simple scheme. The convergence can be accelerated by retaining more information of the left hand side (LHS) of the equation. One method, that in our opinion seems to be very tantalizing, is the so-called diffusion synthetic acceleration (DSA) method.[13] This acceleration method was originally derived for the iterations of the static neutron transport equation. Here, we briefly indicate how this method can be applied to the combined energy and transfer equations of a radiating fluid.

The essence of a diffusion accelerated iteration is to replace the messy spatial transport operator $(\underset{\sim}{\nabla}\cdot\underset{\sim}{P})$ in the combined moment equation [Eq. (I.7)] by the corresponding diffusion equation operator $[\underset{\sim}{\nabla}^2(E/3)]$. By so doing, the <u>difference</u> between the diffusion and the transport operator can be moved to the RHS of the equation. The result is to have a simpler matrix equation to solve (the multigroup diffusion equation), while iterating on the difference between difrusion and transport. In opaque regions, where the diffusion solution is accurate, the transport correction term on the RHS is very small and the iterations converge rapidly. For transparent regions, this type of prescription merely dictates those terms in transport solution on which we should iterate.

In order to use this type of acceleration scheme, we replace Eq. (J.1) with

$$\underset{\sim}{D}_i \underset{\sim}{\psi}_i = \underset{\sim}{R}'_i \quad , \tag{J.2}$$

where

$$\underset{\sim}{R}_i' \equiv \underset{\sim}{R}_i + (\underset{\approx}{D}_i - \underset{\approx}{T}_i)\cdot\underset{\sim}{\psi}_i \quad ,$$

and $\underset{\approx}{D}_i$ is the diffusion matrix operator corresponding to $\underset{\approx}{T}_i$. The grand matrix for the multigroup diffusion equations is shown in Fig. 2. The only difference in form between $\underset{\approx}{D}_i$ and $\underset{\approx}{T}_i$ is that the diagonal matrix blocks corresponding to the cross derivative terms (e.g., $\partial^2/\partial\tau_r\partial\tau_z$) are absent in $\underset{\approx}{D}_i$. Note that since the temperature correction is in both $\underset{\approx}{D}_i$ and $\underset{\approx}{T}_i$, this term stays on the LHS. Also, the term added in the definition of $\underset{\sim}{R}_i'$ involves only the spatial transport operator $\underset{\sim}{\nabla}\cdot\underset{\approx}{P}$. Indeed, since diffusion is really only a special case of the VEF type of solution, this added term is simply

$$(\underset{\approx}{D}_i - \underset{\approx}{T}_i)\cdot\underset{\sim}{\psi}_i = \underset{\sim}{\nabla}\cdot\left[\frac{1}{\gamma+\chi^{n+1}}\left(\underset{\sim}{\nabla}\cdot\underset{\approx}{f}E^{n+1} - \underset{\sim}{\nabla}\frac{E^{n+1}}{3}\right)\right] \quad .$$

In this method, we are iterating on the terms in the radiation pressure tensor that correspond to the anisotropy of the radiation field; just as one would expect as the difference between diffusion and transport.

The solution of Eq. (J.2) is still nontrivial. The main difficulty comes from the fact that we are solving for the temperture simultaneously with the energy densities. Perhaps the best approach is to extend to 2D the split matrix iteration scheme outlined by Axelrod and Dubois.[14] Essentially, the split matrix scheme breaks up $\underset{\approx}{D}_i$ into two matrices, each of which can be solved directly, and alternately moves one part of $\underset{\approx}{D}_i$ to the RHS. For brevity, we shall not comment further about this method, other than to say that since the solution of simplified equation, $\underset{\approx}{D}_i\ \underset{\sim}{\psi}_i = \underset{\sim}{R}_i'$, may require iteration, the iteration on the difference between transport and diffusion is in some sense a secondary iteration and thus may slow the convergence to the transport solution. Trial and error will be necessary to decide which iteration scheme will work best.

IV. CALCULATIONS OF THE VEF TENSOR

In solving the material energy equation for the temperature distribution and the moment equations for the radiation energy density and flux, we assume that the Eddington factors are given. These quantities can be evaluated if we know the full angle-dependence of the radiation field $I(r,z,t,\theta,\phi)$, which must be determined from an angle-by-angle formal solution of the transfer equation for a given distribution of thermal and scattering sources.

We plan to provide several options for calculating the VEF tensor. When examining a particular parameter space, one may choose to use a simpler approximation to a transport type of VEF tensor, leaving the more expensive angle dependent calculations for the final model or for bench-mark problems. These options will span the range from as inexpensive as multigroup (or grey) diffusion to as costly (or hopefully less) as Monte Carlo methods as far as computer time is concerned. In order of computer time expense, these options for the VEF tensor are as follows.

(1) $f^{ij} \equiv \frac{1}{3}\delta^{ij}$ (i.e., multigroup diffusion).

(2) $f^{ij} = [(1 - R_2)/2]\delta^{ij} + [(3R_2 - 1)/2]F^iF^j/F^2$,

where $R_2 = R_2(F/cE)$ is prescribed by a particular theory (e.g., Minerbo[6]); F^i is the ith component of the flux vector and F is its magnitude. We shall discuss this option in more detail below.

(3) An explicit S_n type calculation of the specific intensity to form $\underline{f}$ by angle quadratures. One can use a traditional S_n type formulation here (e.g., TWOTRAN) for a snapshot type Eddington factor. Alternatively, other ray tracing schemes can be developed.[15]

Ray tracing schemes have the advantage of being cheaper than Feautrier type solutions. The main disadvantages of these schemes are: (a) they do not account for retardation effects, as it is unfeasible to store retarded information along the entire

length of a ray, because the total retardation from one end of the ray to another may span several timesteps in the solution. To attempt to handle retardation in this class of schemes would lead to a difficult interpolation problem and a very difficult data management problem. (b) These methods suffer from ray effects. Either the rays may miss an important source volume (long characteristics) or strong local sources may be diffused over the grid by successive interpolations (short characteristics). (c) Because one is computing unidirectional intensities with these methods, it may be difficult to obtain accurate fluxes (which require subtraction of intensities in opposing directions) in opaque regions. This problem is most damaging in the multigroup/grey approach because in either the grey or direct multigroup cases we can evaluate fluxes directly from the moment equations themselves. We shall not discuss these schemes further here.

(4) Finally, one could go to a Feautrier type solution. Here, we choose a set of planes that slice through the cylinder; e.g., each one tangent to one of the radial zones. From the axial symmetry of the problem, it follows that if we know the radiation field on the set of all planes passing through a particular radial zone, then we have all the information needed to determine the azimuthal variation of the radiation field in that zone. On each plane the solution would proceed by forming angle dependent symmetric and antisymmetric averages of the specific intensity, and then effecting a 2D planar solution.[2] Again, further discussion of this method will be given elsewhere.[10]

A. Locally Calculated VEF Tensor

Let us examine option 2 more closely.[16] The purpose of using a locally calculated (i.e., nontransport) Eddington factor prescription is to provide a calculational ability that is more accurate than diffusion, yet nearly as inexpensive.

The prescription given above for $\underline{\underline{f}}$ depends on two quantities: E and $\underline{F}$. In fact, given a scalar and a vector, the

formula uniquely specifies the form of the tensor that is derived from them. Following Minerbo,[6] we write the ratio $R_1 \equiv |\underline{F}|/cE$, so that $R_2 = R_2(R_1)$. In one dimension, R_2 is the Eddington factor, i.e., the ratio of the second to the zeroth angular moment of the radiation field. In two or more dimensions, R_2 is the same ratio, however, the angles are measured relative to the local flux direction. The prescription given above for the tensor $\underline{f}$ then merely maps back to a general coordinate system. Physically, R_2 should be a smooth curve ranging from $R_2(0) = 1/3$ for isotropic radiation to $R_2(1) = 1$ for streaming radiation. (Although there are physical situations for which $f < 1/3$; e.g., a thin plane source of radiation[4] or two concentric opaque shells separated by a vacuum with the outer shell being hotter than the inner one.) The exact form of the curve will be different for each physical situation. However, in using a formula such as Minerbo's[6] for this relation, one is hoping that a variation of the Eddington factor, which has the correct limiting values, will provide a more accurate solution than diffusion.

The main result of Minerbo's paper is the calculation of this relationship between R_2 and R_1. This result is shown in Fig. 3. Three other curves are also shown. The constant value of $R_2 = 1/3$ corresponds to a diffusion calculation. Using a linear expansion of the exponential distribution in his theory, Minerbo also derived a linear approximation for $R_2(R_1)$, referred to as linear in Fig. 3. The final curve in Fig. 3 is the corresponding relationship determined from Levermore and Pomraning's[7] flux-limited diffusion theory. The three <u>variable</u> Eddington factor curves in Fig. 3 span the same general region of this figure between the two limiting values. We have run several idealized test cases to compare these approximate, local formulae for $\underline{f}$ to analytically calculated values. Here we shall present two examples of this type of comparison, one in 1D and one in 2D.

It is critical to note that since the Eddington factor is a function of both the energy density and the flux, these quantities must be calculated self-consistently. Furthermore, since it

is really $\underline{\nabla}\cdot[(\underline{\nabla}\cdot(\underline{f}E)]$ and $\underline{F}$ that enter the dynamical equations for a radiating fluid, the solution of the radiation energy equation (required for self-consistency) depends not only on the value of f, but also on the first and second derivatives of f. Thus, it is not only the value of f predicted by these formulae that is important, but also the shape of the curve.

B. One-Dimensional Test Case

Our first example comparing local prescriptions for Eddington factors is the calculation of the radiation field inside an isothermal sphere. For the case of a constant source function (isothermal, no scattering), it is simple to write down the specific intensity, from which the angular integrals can be generated by numerical quadrature.[15] For this example, we use an optically thin sphere with a radial optical depth of $\tau = 1/2$. The easiest comparison to make is to use the analytically calculated values of E and F to form R_1 and hence obtain f (i.e., not a self-consistent value of f). This comparison is shown in Fig. 4. In this case, the Eddington factor calculated from Minerbo's statistical formula is actually quite close to the real solution. A general trend we have found is also evident here: the values predicted by Levermore's theory and diffusion theory typically bracket the correct values, with a similar dispersion on either side.

In order to have a self-consistent solution, we solve the combined moment equation for the radiation energy density (for more information, see Ref. 16). Here we first make a guess for the energy and flux in a cell, then calculate an Eddington factor from one of the various prescriptions. This Eddington factor is then used in the combined momen equations to calculate a new energy, with which we update the flux and hence Eddington factor and iterate to consistency. Note that the resulting self-consistent solution will not necessarily reproduce the analytically calculated moments of the radiation field. It is precisely this difference in the resulting energy density that we

are trying to find. The results of this calculation for this isothermal sphere are shown in Figs. 5-7. Figure 5 shows the Eddington factors calculated with self-consistent energies and fluxes. This operation moves both the Minerbo and Levermore Eddington factors closer to the analytic solution compared to using only the analytic R_1. However, the linear approximation of Minerbo actually gets worse, with f being a constant 1/3 everywhere. The reason for this behavior is that the linear approximation has a discontinuous second derivative, which results in a numerical feedback problem. It is much better to use a rational polynomial approximation, which has a continuous second derivative, in place of the linear curve.

Figure 6 shows the flux as a function of radius for the self-consistent solution. Minerbo's linear and statistical theories are both very close to the analytic solution, with Levermore's and diffusion spanning each side of the true solution. The energy density and flux calculated from diffusion theory are not in error nearly as much (in most regimes) as the Eddington factor itself; which is another way of stating the well known result that diffusion theory typically works better than it should. Finally, Fig. 7 shows the run of energy density with radius for this test case. These results again show that Minerbo's statistical formulation is the best choice. Diffusion is the worst comparison for this problem (since it is optically thin), with Levermore's formulation being nearly as bad on the other side of the analytic solution. Other 1D test cases are reported in a forthcoming paper.[16]

C. Two-Dimensional Test Case

The two-dimensional test case we present here is that of an an isothermal finite cylinder.[15] We choose the radius of the cylinder to be equal to its height and use an opacity of $\sigma = 0.5\ cm^{-1}$. We have not yet calculated a self-consistent model so we shall show here only the preliminary results for the

Eddington tensor calculated both analytically and with an analytic R_1 used in Minerbo's statistical theory.

There are three independent components of the Eddington tensor f_{rr}, f_{zz} and the off diagonal component f_{rz}. As was the case for the isothermal sphere, the specific intensity is an analytic function.[15] The Eddington tensor can be generated by angle quadratures. The analytic Eddington factors are shown in Fig. 8. Since the source function is everywhere constant, this problem is symmetric about the midplane ($z = 1/2$) as well as around the z axis. The radiation field is nearly isotropic in the center of the cylinder ($f_{ii} = 1/3$, $f_{ij} = 0$). f_{rr} has a different structure than f_{zz} since the optical distance from the center of the cylinder to a boundary is larger in the r-direction than the z-direction. The largest degree of anisotropy of the radiation field (i.e., $f_{rr} \neq f_{zz}$ and $f_{rz} > 0$) is in the corners of the cylinder where points can more easily see both boundaries.

In Fig. 9 we show these same quantities as calculated from Minerbo's statistical arguments. We use the flux and energy density from the analytic solution to form R_1 and thus f. The results in Fig. 9 are given as the difference between Minerbo's and the analytic values. The maximum values of this difference are 0.055 for f_{rr}, 0.04 for f_{rz}, and 0.11 for f_{zz}. These maxima occur near the corners and outer boundary of the cylinder, just where you would expect a non-transport solution to break down. However, especially in 2D, the calculation of the variable Eddington tensor still represents a significant improvement over diffusion. Allowing the main diagonal of the radiation pressure tensor to have non-equal components and allowing for non-zero off diagonal elements at least makes it feasible to describe an anisotropic radiation field to some degree of accuracy (if only locally). These results are very preliminary as we have not done a self-consistent calculation in 2D. However, we hope, as was true for 1D, that in generating the self-consistent solution a) the solution converges, and b) the Eddington factors will approach the analytic values.

REFERENCES

1. K.D. Lathrop and F.W. Brinkley, Jr., "TWOTRAN-II: An Interfaced, Exportable Version of the TWOTRAN Code for Two-Dimensional Transport," Los Alamos National Laboratory Report LA-4848-MS (July 1973).

2. D. Mihalas, L.H. Auer, and B.R. Mihalas, Astrophys. J., 220, 1001, (1978).

3. This concept is an extension of the variable Eddington approximation in 1D. For 1D cases see, e.g., "The VERA System of Radiation Hydrodynamics Codes," Vol. 1. System, Science and Software Report DASA 2258-1 (1969). La Jolla, California: P.O. Box 1620.

4. D. Mihalas, Stellar Atmospheres, 2nd Ed., W.H. Freeman and Co., San Francisco (1978).

5. D.S. Kershaw, J. Comp Phys., 39, 375 (1981).

6. G.N. Minerbo, J. Quant. Spectrosc. and Rad. Transfer, 20, 541, (1978).

7. C. D. Levermore, and G.C. Pomraning, Astrophys. J., 248, 321, (1981).

8. L.H. Auer, J. Quant. Spectrosc. and Rad. Transfer, 11, 573, (1971).

9. D. Mihalas and R. Weaver, J. Quant. Spectrosc. and Rad. Transfer, in press (1982).

10. D. Mihalas, R. Weaver, and G. Olson, "Two Dimensional Cylindrical Radiation Transfer," Los Alamos National Laboratory Repo t, in preparation.

11. D. Mihalas, R. Weaver, and J. Sanderson, J. Quant. Spectrosc. and Rad. Transfer, in press (1982).

12. B.E. Freeman and L.E. Hauser, "A New Method for Solving the 1-D VERA Equations: The Multifrequency/grey Technique," System, Science and Software report, No. 3SIR-38, La Jolla, California: P.O. Box 1620, (1969).

13. R.E. Alcouffe, Nuc. Sci. and Eng., 64, 344 (1977).

14. T.A. Axelrod, and P.F. Dubois, 1980 unpublished.

REFERENCES (cont'd)

15. P.M. Campbell, 1971 "Two Dimensional Characteristic Ray Code Development," DASA Report No. 2605.

16. G. Olson, R.P. Weaver, and D. Mihalas, 1982 "One Dimensional, Eddington Factor Calculations," Los Alamos National Laboratory, in preparation.

Figure 1. A schematic diagram of the form of the grand matrix to be solved in the full multigroup, 2D combined moment and material energy equation. The matrix shown is for I = J = 4. The main block diagonal is composed of arrow matrices, which have a simple decomposition.

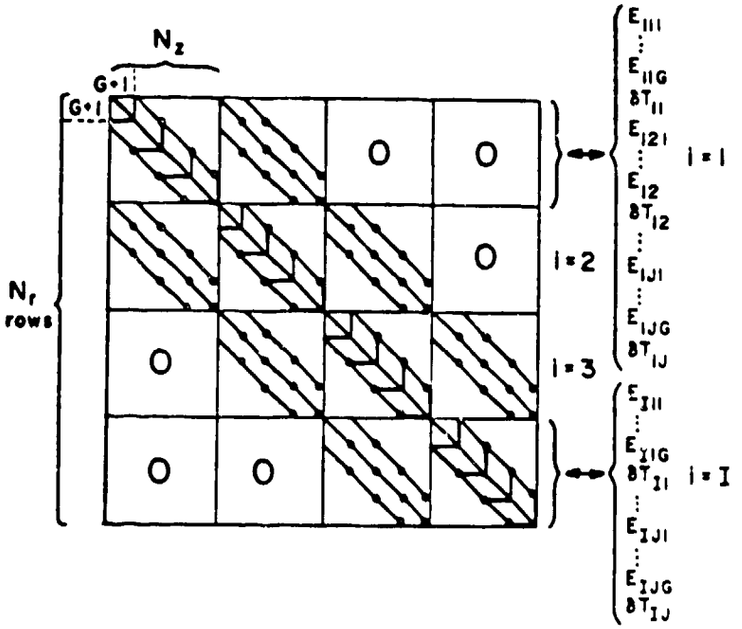

Figure 2. Same as Fig. 1, except for the full multigroup diffusion equation in place of the transport equation.

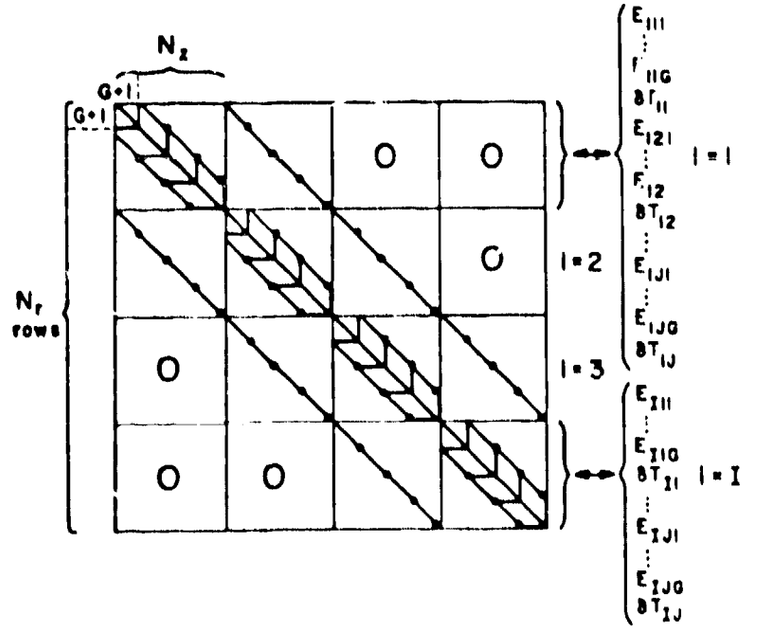

Figure 3. Functional forms for the moment relationship $R_2(R_1)$ for various theories. Here, $m_i \equiv \int \mu^i I(\mu,\nu,d\omega$ is the ith moment of the radiation specific intensity. In 1D, $R_2 = f$, the Eddington factor.

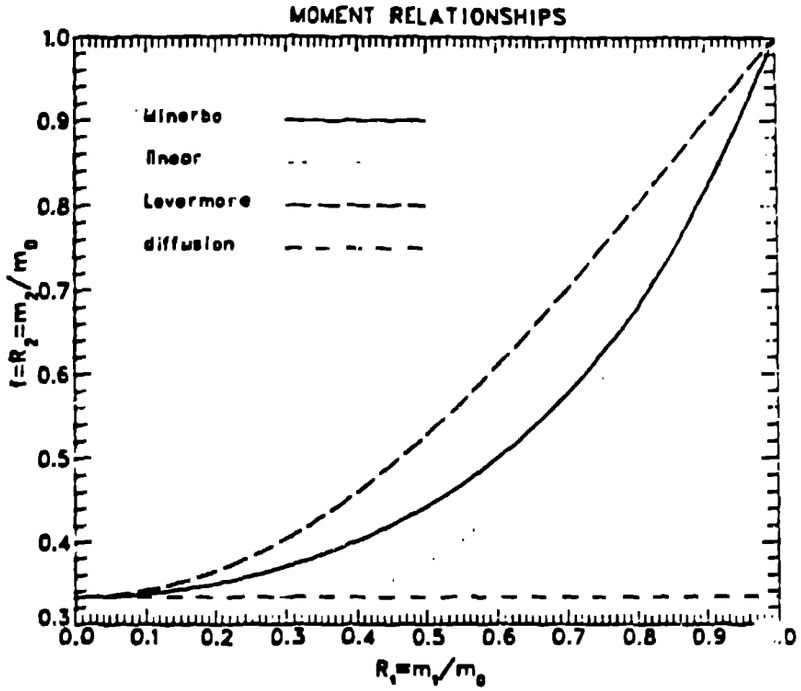

Figure 4. The calculated Eddington factors versus radius for an isothermal sphere with a radial optical depth of 0.5. The Eddington factor is calculated locally from the analytic values of $R_1 \equiv F/cE$ for various theories.

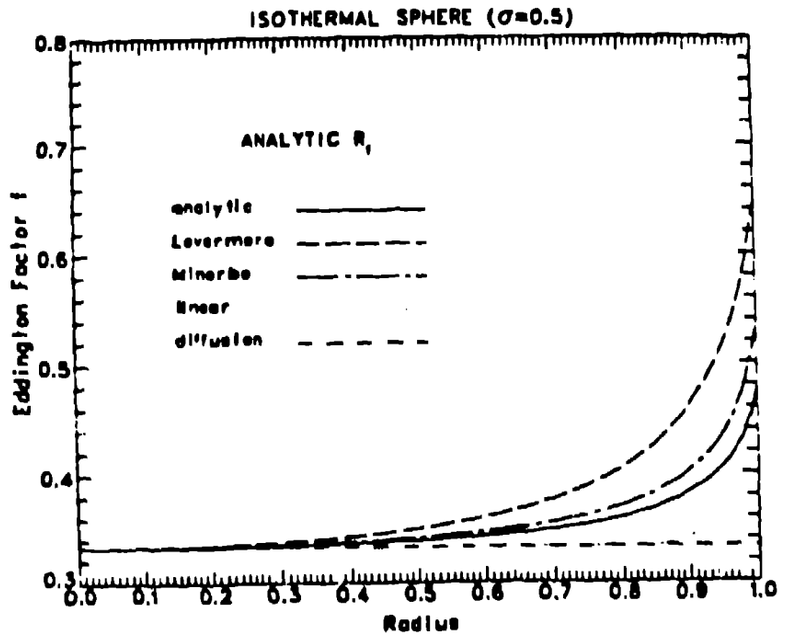

Figure 5. The calculated Eddington factors from a self consistent solution of the combined moment equation for the problem described in Fig. 4.

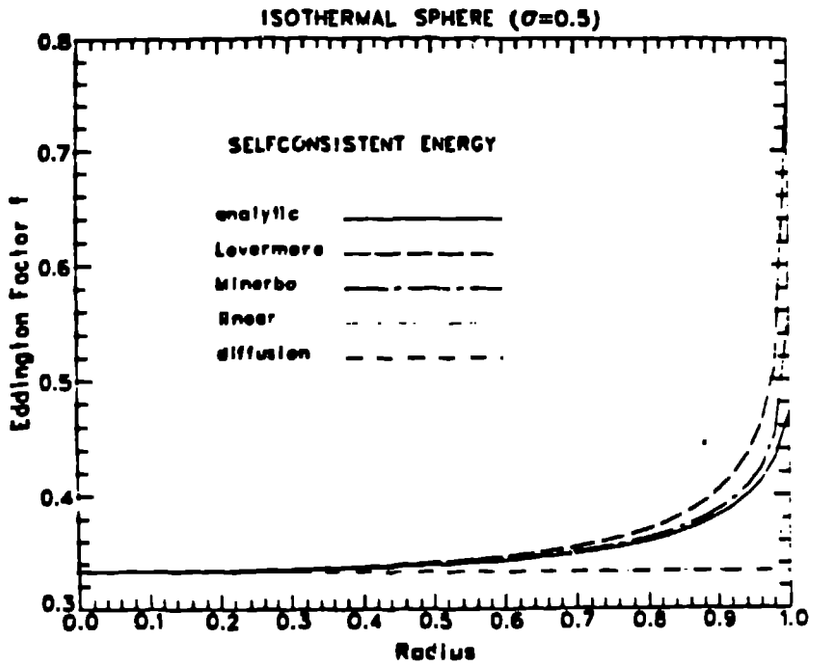

Figure 6. The calculated fluxes from a self consistent solution of the combined moment equation for the problem described in Fig. 4.

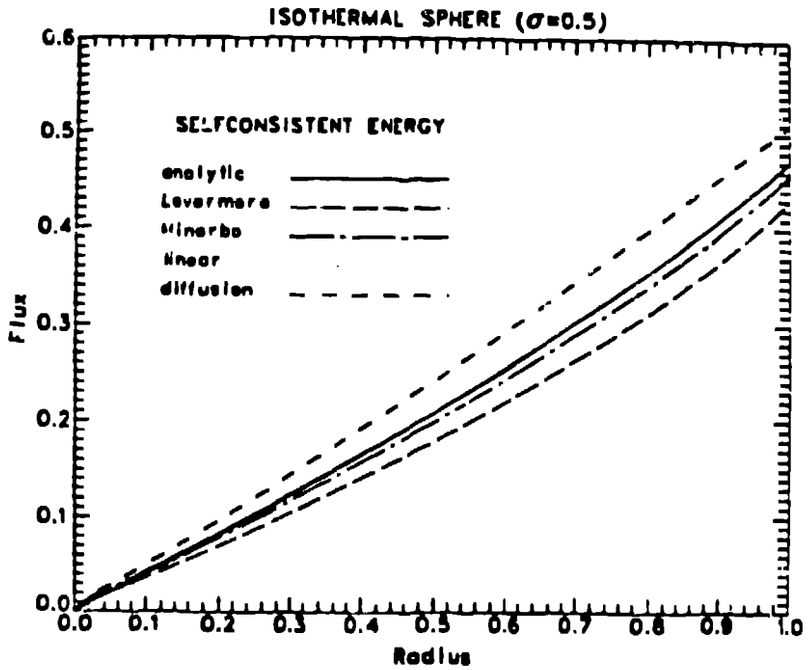

Figure 7. The calculated energy densities from a self consistent solution of the combined moment equation for the problem described in Fig. 4.

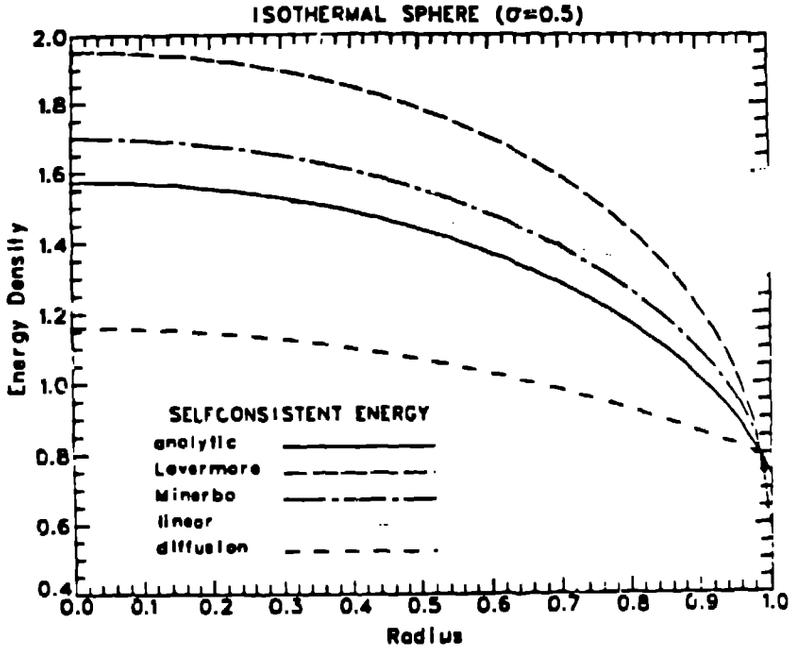

Figure 8. A contour plot of the analytic Eddington factors f_{rr}, f_{zz}, and f_{rz} for an isothermal cylinder with a radius equal to its height. The opacity inside the cylinder is $S = 0.5\ cm^{-1}$.

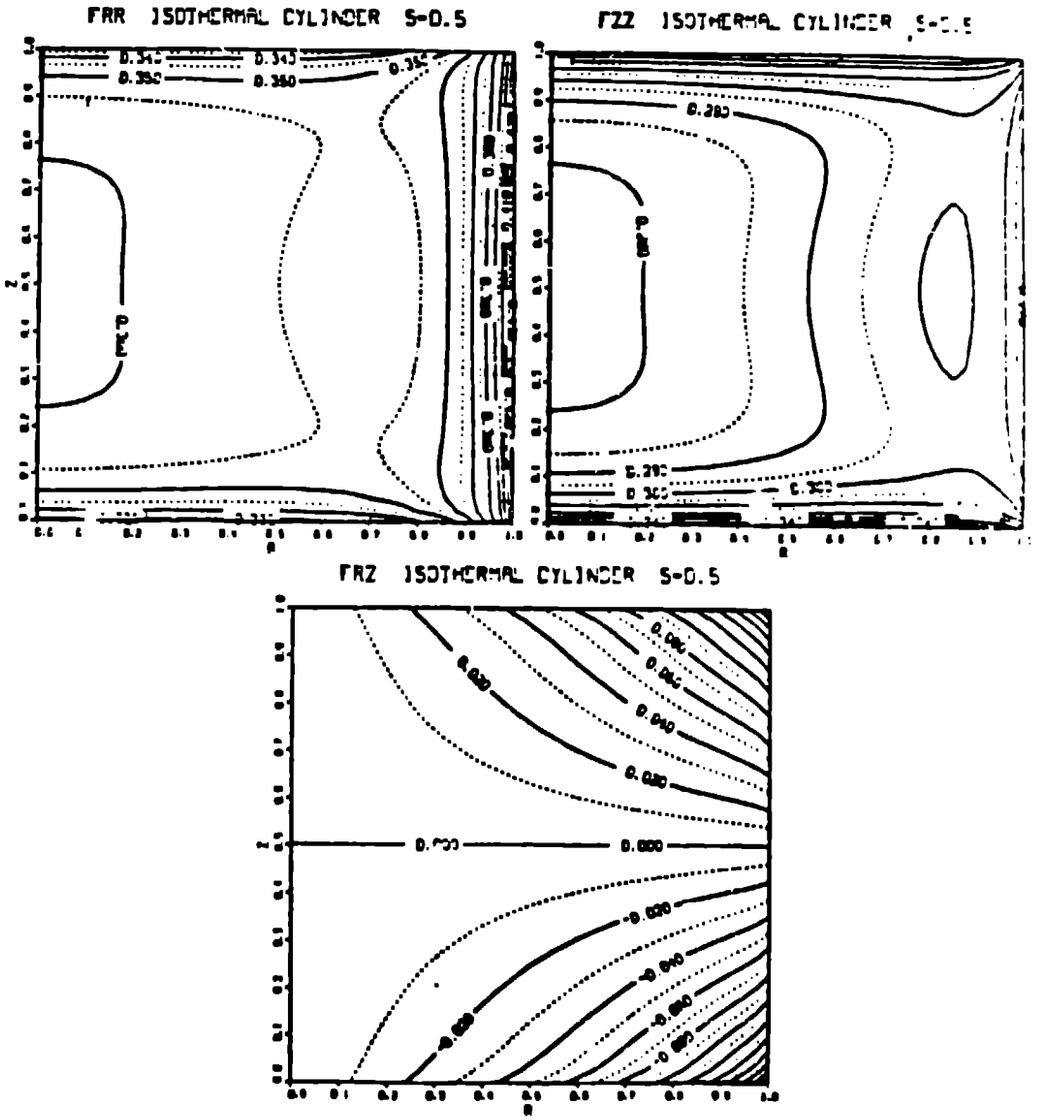

Figure 9. The difference between the Minerbo theory and the analytic Eddington factors for the isothermal cylinder described in Fig. 8. An analytic R_1 is used in Minerbo's theory; thus, these results are not self consistent.